JACS
JOURNAL OF THE AMERICAN CHEMICAL SOCIETY
Communication
pubs.acs.org/JACS

Hierarchically Porous Polymer Monoliths by Combining Controlled Macro- and Microphase Separation

Stacey A. Saba,[†] Maral P. S. Mousavi,[‡] Philippe Bühlmann,[‡] and Marc A. Hillmyer*[,‡]

[†]Department of Chemical Engineering and Materials Science and [‡]Department of Chemistry, University of Minnesota, Minneapolis, Minnesota 55455-0431, United States

Supporting Information

ABSTRACT: The ability to tune polymer monolith porosity on multiple length scales is desirable for applications in liquid separations, catalysis, and bioengineering. To this end, we have developed a facile synthetic route to nanoporous polymer monoliths based on controlled polymerization of styrene and divinylbenzene from a poly(lactide) macro-chain transfer agent in the presence of nonreactive poly(ethylene oxide) (PEO). Simple variations in the volume fraction and/or molar mass of PEO lead to either polymerization-induced microphase separation or simultaneous macro- and microphase separation. These processes dictate the resultant morphology and allow for control of the macro- and microstructure of the monoliths. Subsequent selective etching produces monoliths with morphologies that can be tailored from mesoporous, with control over mesopore size, to hierarchically meso- and macroporous, with percolating macropores. This convenient synthetic route to porous polymer monoliths has the potential to be useful in applications where both rapid mass transport and a high surface area are required.

Hierarchically porous monoliths with a percolating macroporous (>50 nm) network[1,2] and accessible mesopores (2−50 nm) are useful materials for liquid separations,[3,4] catalysis,[5] and biomedical applications.[6] Furthermore, the ability to tune the mesopore size enables size-selective filtration applications.[7,8] There are examples of such hierarchically porous carbons[9−11] and other inorganic materials,[12,13] but the development of synthetic routes to controlled pore sizes in such hierarchically porous polymers has been limited.[14−17] Most reports of hierarchically porous polymers with both meso- and macropores have focused on uncontrolled free radical polymerizations[18,19] or thin-layer membrane fabrication.[20−22] Here, we report the facile controlled synthesis of porous polymer monoliths, and the ability to tune the nanostructure of the monolith from mesoporous to hierarchically porous, with percolating macropores. The versatility of this technique allows for ready tailoring of the mesopore size distribution.

Previously, Seo and Hillmyer reported the use of polymerization-induced microphase separation to prepare nanostructured polymer monoliths with interconnected mesopores.[23] The structure was generated using reversible addition−fragmentation chain transfer (RAFT) copolymerization of styrene (S) and divinylbenzene (DVB) from a poly(lactide) macro-chain transfer agent (PLA-CTA), during which *in situ* cross-linking trapped the disordered bicontinuous structure. Successive hydrolysis of the PLA domains produced nanoporous P(S-*co*-DVB). Subsequent work demonstrated the versatility of this approach through the introduction of a nonreactive functional additive that selectively swells a single domain of the block polymer while retaining the microphase-separated morphology.[24,25] Polymerization-induced formation of macroporosity in related systems is also well established; in this approach a nonreactive additive, such as a small molecule[26,27] or polymer,[28] is dissolved in a multifunctional monomer mixture. The additive is chosen to be insoluble in the polymer, resulting in polymerization-induced macrophase separation of the polymer from the additive. Removal of the additive or porogen can produce an interconnected macroporous polymer monolith.

Here we report a new hybrid approach to prepare porous polymer monoliths via the copolymerization of S and DVB from PLA-CTA in the presence of a nonreactive poly(ethylene oxide) (PEO) additive, as depicted in Figure 1. PEO is soluble in S and DVB monomers, and its miscibility with PLA allows for the formation of PLA/PEO composite domains in linear blends of PS-*b*-PEO/PS-*b*-PLA.[29] In this work, we show that by restricting domain size via *in situ* cross-linking, the PLA domains cannot accommodate all compositions of PEO. At high molar mass, the PEO macrophase separates from the *in situ* formed PLA-*b*-P(S-*co*-DVB), leading to macroscopic features on the order of hundreds of nanometers. For all compositions, soaking the monolith in water allows for selective extraction of the PEO, and treatment with aqueous solutions of base results in removal of both the PLA and the PEO, producing a hierarchically porous polymer monolith. A typical reaction mixture composed of 26 vol % PLA-CTA (31 kg mol^{-1}) dissolved in a 4/1 molar mixture of S/DVB was combined with PEOs (30−70 vol % overall) of varying molar mass (5, 20, and 35 kg mol^{-1}). Simply heating for 20 h at 120 °C produced nanostructured polymer monoliths. By varying the molar mass and volume fraction of the PEO additive, the monolith morphology was easily tuned from mesoporous, with adjustable mean pore size, to hierarchically porous.

Before removal of the PLA and PEO from the nanostructured monoliths, small-angle X-ray scattering (SAXS) indicated compositional heterogeneities on the order of 20−50 nm. Broad principal scattering peaks in all samples are

Received: May 13, 2015
Published: July 10, 2015

DOI: 10.1021/jacs.5b04992
J. Am. Chem. Soc. 2015, 137, 8896−8899

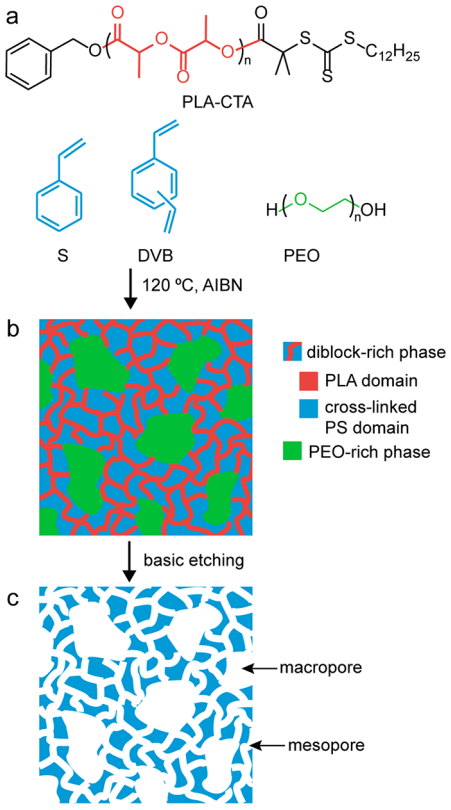

Figure 1. Preparation of hierarchically porous polymer monoliths. (a) The reaction mixture consists of PLA-CTA and PEO additive dissolved in S and DVB. (b) RAFT copolymerization is used to generate a PLA-*b*-P(S-*co*-DVB) diblock polymer. As a result of the copolymerization, the nonreactive PEO additive macrophase separates from the microphase-separated diblock polymer. (c) Etching in basic solution simultaneously degrades the PLA and dissolves the PEO, producing mesopores and macropores, respectively.

characteristic of a disordered microphase-separated block polymer. The shift of peak maxima toward low angle with increasing volume fraction of PEO is typical of blends of a diblock and homopolymer, indicating a shift toward macrophase separation (Figure S1a).[30] In all the as-prepared monoliths, melting endotherms were observed upon heating by differential scanning calorimetry (DSC), consistent with incorporation of semicrystalline PEO into the monoliths (Figure S2a). Subsequent removal of the PLA and the majority of the PEO was confirmed with Fourier transform infrared spectroscopy and by gravimetric analysis. In all cases, the characteristic carbonyl stretching band of the PLA (1755 cm^{-1}) was absent after the etching step (Figure S3). Furthermore, the nanostructural integrity was retained after etching and resulted in nanoporous polymer monoliths, as evidenced by SAXS. Corresponding SAXS patterns for the porous monoliths exhibited no change in the position of the principal scattering peak when compared to the unetched precursors, and the increased scattering intensity is consistent with increased electron density contrast between the voids and the P(S-*co*-DVB) (Figure S1b). DSC thermograms of the etched monoliths showed a smaller melting endotherm, compared to the unetched precursors, due to low levels of trapped PEO in the cross-linked PS matrix (Figure S2b). Interestingly, the presence of residual PEO in the cross-linked PS matrix improved the wettability of the monolith, compared to monoliths prepared without any PEO additive. For example, monoliths with residual PEO were able to uptake water, as confirmed gravimetrically and by a dying experiment, while porous cross-linked PS were not (Figure S4).

The morphology of the porous monoliths was further characterized by scanning electron microscopy (SEM) and nitrogen sorption experiments. When varying amounts of 5 kg mol^{-1} PEO additive were introduced into the reaction mixture, the PEO swelled the PLA domains of the resulting cross-linked, nanostructured monolith. In these cases, SEM micrographs show that the resultant etched monoliths consist of a disordered mesoporous structure with no evidence of macrophase separation (Figures 2 and S5). Nitrogen sorption

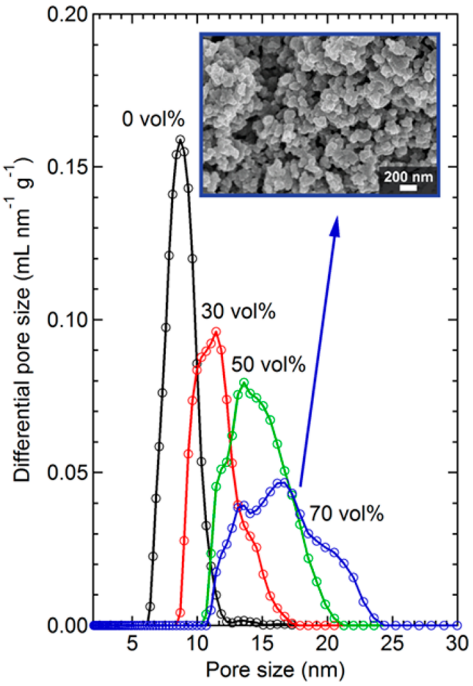

Figure 2. Mesopore size distributions based on QSDFT analysis of the adsorption branch for monoliths prepared with different volume fractions (black: 0, red: 30, green: 50, blue: 70 vol %) of 5 kg mol^{-1} PEO additive. Inset: SEM micrograph of an etched monolith prepared with 70 vol % of 5 kg mol^{-1} PEO additive. The sample was coated with ~3 nm of Pt prior to imaging.

experiments gave type IV isotherms with H2 hysteresis, characteristic of disordered mesoporous materials (Figure S6).[31] These data are similar to that obtained in monoliths prepared without any PEO (Figure S7).[23] However, increasing the PEO content leads to increased swelling of the PLA domains, as evidenced by an increase in mean pore size for the corresponding etched samples. Mesopore size distributions were estimated based on a quenched solid density functional theory (QSDFT) kernel applied to the adsorption branch using a cylindrical pore model (Figure 2).[32] The average pore sizes are 7, 11, 14, and 17 nm, and the specific surface areas, based on Brunauer–Emmett–Teller (BET) analysis, are 220, 134, 120, and 88 m^2 g^{-1} for monoliths derived from 0, 30, 50, and 70 vol % PEO, respectively.[33] Independent of the amount of added 5 kg mol^{-1} PEO, the microphase-separated structure is trapped via *in situ* cross-linking. This affords control over mesopore size and accesses pore sizes larger than those prepared without any

DOI: 10.1021/jacs.5b04992
J. Am. Chem. Soc. 2015, 137, 8896–8899

additive using a single PLA-CTA,[23] which is desirable for applications requiring tailored size selectivity.[34]

Increasing the molar mass of the PEO additive to 20 kg mol^{-1} at 30 vol % results in both macro- and microphase separation. SEM micrographs suggest that the structure contains isolated macropores that are accessible through a percolating mesoporous network (Figures 3a,b and S8), which

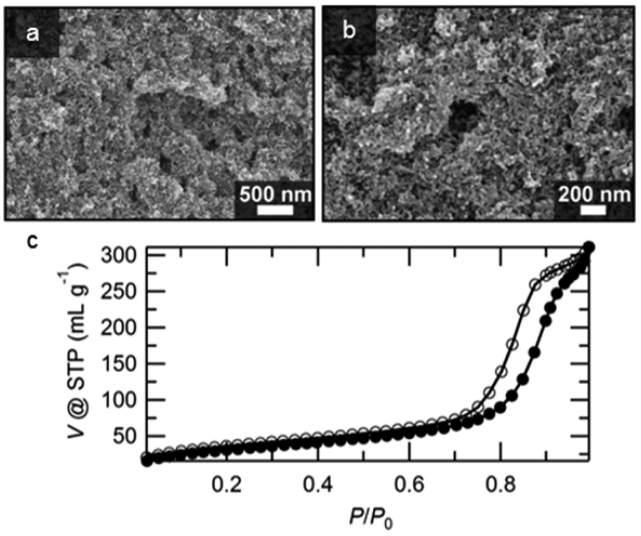

Figure 3. SEM micrographs at (a) 25,000× and (b) 50,000× magnification and (c) nitrogen sorption isotherm of an etched monolith prepared with 30 vol % of 20 kg mol^{-1} PEO additive. Filled circles (●) indicate adsorption and open circles (○) indicate desorption.

is consistent with the opaque white appearance of the sample due to the scattering of visible light. Hierarchical porosity was further confirmed by nitrogen sorption analysis (Figure 3c). The hysteresis step at P/P_0 = 0.75−0.90 is associated with capillary condensation and evaporation in the mesopores, and the step at P/P_0 > 0.98 indicates the filling of macropores. This monolith has a BET specific surface area of 115 m^2 g^{-1} and a QSDFT average pore size of 11 nm, consistent with other related mesoporous polymeric materials.[23] Further increasing the 20 kg mol^{-1} PEO additive to 50 vol % resulted in an increase in the apparent connectivity of the macropores, which is consistent with the increase in volume fraction of the pore-forming component (Figure S9). The mesostructure was retained in this monolith as well, with a QSDFT average pore size of 11 nm and a BET specific surface area of 103 m^2 g^{-1}. The cross-linked polymer formed a globular structure with macropores composed of voids between the globules and mesopores located within the globules. Interestingly, this globular morphology is often observed when the nonreactive additive is a small molecule.[35]

Further increasing the molar mass of the PEO additive to 35 kg mol^{-1} resulted in a dramatic morphological change. Macropores with sizes on the order 0.1−0.3 μm were observed along with mesopores in the macroporous framework (Figures 4, S10, and S11). The BET specific surface areas are 93 and 77 m^2 g^{-1} for 30 and 50 vol % of 35 kg mol^{-1} PEO additive, respectively. Both monoliths have QSDFT average pore sizes of 10 nm. The residual PEO content in a monolith prepared in the presence of 50 vol % of 35 kg mol^{-1} PEO was determined by ^{1}H NMR spectroscopy by immersing the etched monolith in

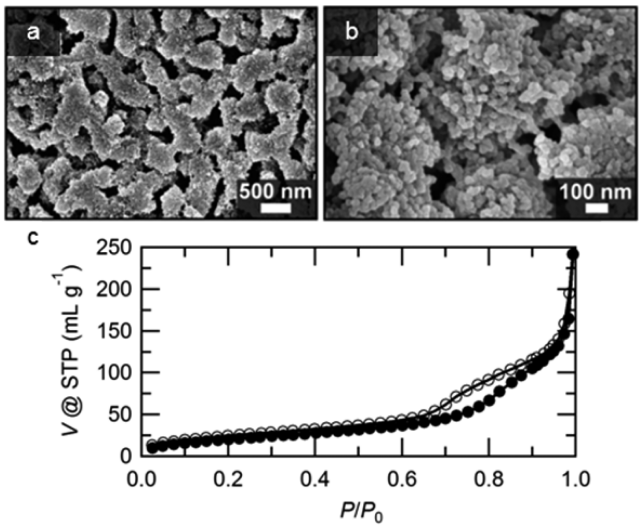

Figure 4. Morphology of a hierarchically porous polymer after etching, derived from a monolith prepared with 50 vol % of 35 kg mol^{-1} PEO additive. SEM micrographs at magnifications of (a) 25,000× and (b) 90,000×, and (c) the corresponding nitrogen sorption isotherm. Filled circles (●) correspond to the adsorption branch, and the open circles (○) to the desorption branch.

deuterated chloroform with an internal standard. This process extracted the residual 11 ± 1 wt % PEO (Figure S12). Additionally, macrophase separation of the PEO from the diblock was confirmed by soaking a monolith in deionized water with no base. This resulted in a monolith with only macropores and a much lower BET specific surface area of 23 m^2 g^{-1} (Figure S13).

We further analyzed a monolith derived from 50 vol % 35 kg mol^{-1} PEO to determine the continuity of the macropores. Based on gravimetric analysis, the majority of the PEO was removed during etching, which suggests that the majority of the macropores are accessible to water. The accessibility of the macropores was confirmed by time-resolved impedance spectroscopy (Figure S14). Bulk impedance measurements were made periodically over the course of 70 h on precursor monoliths exposed to 1.0 mM KCl aqueous solution. The data were then fit to obtain bulk resistance. The high initial resistance (>1 MΩ) is due to the hindrance of electrical charge transfer across the dense nonporous monolith. Over time, the resistance drops as the PEO is extracted and the macropores are formed, and reaches a constant value of 610 kΩ after approximately 8 h. The resistance of the monolith was comparable to that of a nanoporous glass plug with a percolating pore network and identical dimensions (372 kΩ when filled with 1.0 mM KCl).[36,37]

In this work, we have discovered a route to mesoporous and hierarchically meso- and macroporous polymer monoliths with tunable morphology and controllable pore size by combining macro- and microphase separation. The nanostructures were characterized by SAXS, SEM, and nitrogen sorption, and the wettability of the monoliths is well suited for applications in aqueous solution. The starting materials are readily available, and the synthetic ease is advantageous. We have now attained a unique combination of control over pore size and synthetic simplicity in the production of hierarchically porous monoliths with large pores and high surface area. We envision that such structures could be useful in applications requiring both rapid mass transport and selectivity.

DOI: 10.1021/jacs.5b04992
J. Am. Chem. Soc. 2015, 137, 8896−8899

■ ASSOCIATED CONTENT

Supporting Information

Experimental details and characterization data. The Supporting Information is available free of charge on the ACS Publications website at DOI: 10.1021/jacs.5b04992.

■ AUTHOR INFORMATION

Corresponding Author

*hillmyer@umn.edu

Notes

The authors declare no competing financial interest.

■ ACKNOWLEDGMENTS

The authors thank Morgan Schulze and Dr. Jonathan Hollinger for helpful discussions, and Dr. Justin Bolton for synthesis of the RAFT agent. This work was supported by the National Science Foundation (DMR-1006370). S.A.S. acknowledges support from the NSF Graduate Research Fellowship Program (GRFP) and M.P.S.M. is supported by a UMN Doctoral Dissertation Fellowship. Parts of this work were carried out in the Characterization Facility, University of Minnesota, which receives partial support from NSF through the MRSEC program. Portions of this work were performed at the DuPont-Northwestern-Dow Collaborative Access Team (DND-CAT) located at Sector 5 of the Advanced Photon Source. DND-CAT is supported by the E.I. DuPont de Nemours & Co., The Dow Chemical Company, the U.S. National Science Foundation through Grant DMR-9304725 and the State of Illinois through the Department of Commerce and the Board of Higher Education Grant IBHE HECA NWU 96. Use of Advanced Photon Source was supported by the U.S. Department of Energy, Office of Science, Office of Basic Energy Science, under contract no. W-31-109-Eng 38.

■ REFERENCES

(1) Hjertén, S.; Liao, J.-L.; Zhang, R. *J. Chromatogr.* **1989**, *473*, 273−275.

(2) Svec, F.; Fréchet, J. M. J. *Anal. Chem.* **1992**, *64*, 820−822.

(3) Shintani, Y.; Zhou, X.; Furuno, M.; Minakuchi, H.; Nakanishi, K. *J. Chromatogr. A* **2003**, *985*, 351−357.

(4) Sinner, F.; Buchmeiser, M. R. *Macromolecules* **2000**, *33*, 5777−5786.

(5) Bronstein, L. M.; Goerigk, G.; Kostylev, M.; Pink, M.; Khotina, I. A.; Valetsky, P. M.; Matveeva, V. G.; Sulman, E. M.; Sulman, M. G.; Bykov, A. V.; Lakina, N. V.; Spontak, R. J. *J. Phys. Chem. B* **2004**, *108*, 18234−18242.

(6) He, L.; Zhang, Y.; Zeng, C.; Ngiam, M.; Liao, S.; Quan, D.; Zeng, Y.; Lu, J.; Ramakrishna, S. *Tissue Eng., Part C* **2009**, *15*, 243−255.

(7) Mulvenna, R. A.; Weidman, J. L.; Jing, B.; Pople, J. A.; Zhu, Y.; Boudouris, B. W.; Phillip, W. A. *J. Membr. Sci.* **2014**, *470*, 246−256.

(8) Li, L.; Schulte, L.; Clausen, L. D.; Hansen, K. M.; Jonsson, G. E.; Ndoni, S. *ACS Nano* **2011**, *5*, 7754−7766.

(9) Taguchi, A.; Smätt, J. H.; Lindén, M. *Adv. Mater.* **2003**, *15*, 1209−1211.

(10) Wang, Z.; Li, F.; Ergang, N. S.; Stein, A. *Chem. Mater.* **2006**, *18*, 5543−5553.

(11) Liang, C.; Dai, S. *Chem. Mater.* **2009**, *21*, 2115−2124.

(12) Minakuchi, H.; Nakanishi, K.; Soga, N.; Ishizuka, N.; Tanaka, N. *Anal. Chem.* **1996**, *68*, 3498−3501.

(13) Smått, J.-H.; Weidenthaler, C.; Rosenholm, J. B.; Linden, M. *Chem. Mater.* **2006**, *18*, 1443−1450.

(14) Seo, M.; Kim, S.; Oh, J.; Kim, S.-J.; Hillmyer, M. A. *J. Am. Chem. Soc.* **2015**, *137*, 600−603.

(15) Maya, F.; Svec, F. *Polymer* **2014**, *55*, 340−346.

(16) Valkama, S.; Nykänen, A.; Kosonen, H.; Ramani, R.; Tuomisto, F.; Engelhardt, P.; Ten Brinke, G.; Ikkala, O.; Ruokolainen. *Adv. Funct. Mater.* **2007**, *17*, 183−190.

(17) Jones, B. H.; Lodge, T. P. *ACS Nano* **2011**, *5*, 8914−8927.

(18) Li, Y.; Tolley, H. D.; Lee, M. L. *J. Chromatogr. A* **2010**, *1217*, 8181−8185.

(19) Lubbad, S. H.; Buchmeiser, M. R. *J. Sep. Sci.* **2009**, *32*, 2521−2529.

(20) Sai, H.; Tan, K. W.; Hur, K.; Asenath-Smith, E.; Hovden, R.; Jiang, Y.; Riccio, M.; Muller, D. A.; Elser, V.; Estroff, L. A.; Gruner, S. M.; Wiesner, U. *Science* **2013**, *341*, 530−534.

(21) Hess, S. C.; Kohll, A. X.; Raso, R. A.; Schumacher, C. M.; Grass, R. N.; Stark, W. J. *ACS Appl. Mater. Interfaces* **2015**, *7*, 611−617.

(22) Bolton, J.; Bailey, T. S.; Rzayev, J. *Nano Lett.* **2011**, *11*, 998−1001.

(23) Seo, M.; Hillmyer, M. A. *Science* **2012**, *336*, 1422−1425.

(24) Schulze, M. W.; McIntosh, L. D.; Hillmyer, M. A.; Lodge, T. P. *Nano Lett.* **2014**, *14*, 122−126.

(25) McIntosh, L. D.; Schulze, M. W.; Irwin, M. T.; Hillmyer, M. A.; Lodge, T. P. *Macromolecules* **2015**, *48*, 1418−1428.

(26) Viklund, C.; Svec, F.; Fréchet, J. M. J.; Irgum, K. *Chem. Mater.* **1996**, *8*, 744−750.

(27) Moravcová, D.; Jandera, P.; Urban, J.; Planeta, J. *J. Sep. Sci.* **2003**, *26*, 1005−1016.

(28) Kanamori, K.; Hasegawa, J.; Nakanishi, K.; Hanada, T. *Macromolecules* **2008**, *41*, 7186−7193.

(29) Mao, H.; Hillmyer, M. A. *Macromol. Chem. Phys.* **2008**, *209*, 1647−1656.

(30) Roe, R. J.; Nojima, S. *Mater. Res. Soc. Symp. Proc.* **1987**, *79*, 151−158.

(31) Lowell, S.; Shields, J. E.; Thomas, M. A.; Thommes, M. *Characterization of Porous Solids and Powders: Surface Area, Pore Size and Density*; Scarlett, B., Ed.; Kluwer Academic Publishers: Norwell, MA, 2004; pp 13, 44.

(32) Gor, G. Y.; Thommes, M.; Cychosz, K. A.; Neimark, A. V. *Carbon* **2012**, *50*, 1583−1590.

(33) Brunauer, S.; Emmett, P. H.; Teller, E. *J. Am. Chem. Soc.* **1938**, *60*, 309−319.

(34) Viklund, C.; Nordström, A.; Irgum, K.; Svec, F.; Fréchet, J. M. J. *Macromolecules* **2001**, *34*, 4361−4369.

(35) Barlow (née Tan), K. J.; Hao, X.; Hughes, T. C.; Hutt, O. E.; Polyzos, A.; Turner, K. A.; Moad, G. *Polym. Chem.* **2014**, *5*, 722−732.

(36) Mousavi, M. P. S.; Bühlmann, P. *Anal. Chem.* **2013**, *85*, 8895−8901.

(37) *CoralPor Porous Glass Product Information*. http://www.us.schott.com. Accessed on May 8, 2015.

DOI: 10.1021/jacs.5b04992
J. Am. Chem. Soc. 2015, 137, 8896−8899